IMF-driven plasmasphere erosion of 10 July 2000

J. Goldstein,[1] B. R. Sandel,[2] W. T. Forrester,[2] and P. H. Reiff[1]

Received 18 October 2002; revised 21 November 2002; accepted 23 December 2002; published 14 February 2003.

[1] On 10 July 2000, the IMAGE EUV imager observed erosion of the nightside plasmasphere that occurred in two bursts during 5–8 UT. The plasmapause radial velocity V_{pp} at 2.4 MLT was extracted from the time sequence of EUV images. We show that intervals of $V_{pp} < 0$ (i.e., erosion) are correlated with intervals of southward (S_{wd}) interplanetary magnetic field (IMF), if the solar wind and IMF data are time-delayed by 30 minutes (in addition to a 3.7-minute delay for propagation to the magnetopause). This suggests that coupling between the solar wind and the plasmapause, involving processes in the ionosphere and magnetotail, takes about 30 minutes. A 6:40 UT magnetosphere compression may have hurried the onset of the second erosion. *INDEX TERMS:* 2768 Magnetospheric Physics: Plasmasphere; 2730 Magnetosphere—inner; 2784 Solar wind/magnetosphere interactions; 2712 Electric fields (2411); 2740 Magnetospheric configuration and dynamics. **Citation:** Goldstein, J., B. R. Sandel, W. T. Forrester, and P. H. Reiff, IMF-driven plasmasphere erosion of 10 July 2000, *Geophys. Res. Lett.*, *30*(3), 1146, doi:10.1029/2002GL016478, 2003.

1. Introduction

[2] The plasmapause is the outer boundary of the Earth's plasmasphere, a torus-shaped region of the inner magnetosphere containing cold, relatively dense ($\gtrsim$100 cm^{-3}) plasma. To explain why the size of the plasmasphere (i.e., the radial location of the plasmapause) varies inversely with geomagnetic activity, *Nishida* [1966] and *Brice* [1967] proposed a simple picture involving the interplay between the magnetospheric convection field (induced by the flow of the solar wind past the magnetosphere) and the coupling of high-altitude plasma to the Earth's corotating ionosphere. Active periods trigger plasmaspheric erosion, in which the outer layers of the plasmasphere are stripped away by enhanced convection, and the plasmapause moves inward, producing a smaller plasmasphere. One refinement to this picture is the shielding effect. In response to enhanced convection, the earthward edge of the plasmasheet forms partial ring currents (RC) that are completed in the ionosphere; finite ionospheric conductivity creates an electric field that shields the inner magnetosphere from convection. Because the shielding layer takes a finite time ($\lesssim$1 hr [*Kelley et al.*, 1979]) to adjust, a sudden convection increase can penetrate past the shielding layer and erode the plasmasphere. A key contribution to the erosion process may come from intense azimuthal flows dubbed 'sub-auroral polarization streams' (SAPS) [*Foster and Burke*, 2002]. SAPS arise via coupling between the ring current and low-conductivity ionosphere regions, and (on average) are strongest in pre-midnight magnetic local time (MLT) during storms.

[3] There have been many non-global measurements of variations in the plasmapause radius with time (see [*Lemaire and Gringauz*, 1998] and references therein); e.g., polar satellite plasmapause crossings on a time scale of tens of minutes to a couple of hours, and whistler measurements of cross-*L* drifts. Due to the elusiveness of direct observations of the formation of a new plasmapause, important questions have remained unanswered about the details of the erosion process and its effects on the plasmapause [*Richmond*, 1973; *Huang et al.*, 1990; *LeDocq et al.*, 1994; *Carpenter*, 1995; *Moldwin et al.*, 1995]. Models for time-dependent position of the plasmapause have been created, both empirical (e.g., *Carpenter and Anderson* [1992]) and computational (e.g., *Chen and Wolf* [1972]; *Lambour et al.* [1997]). Often these models are (at least in part) based on average (i.e., statistical) properties deduced from in situ and/or ground-based data. Simulations can use somewhat arbitrary or unrealistic assumptions for initial and/or boundary conditions. Historically it has been a challenge to reconcile the results of these models with sparse satellite coverage of the plasmasphere.

[4] Recent advances in satellite-based imaging techniques have made it possible to routinely obtain full global images of the plasmasphere. The IMAGE satellite's extreme ultraviolet (EUV) imager [*Sandel et al.*, 2000], which detects 30.4-nm emissions of the helium portion of the plasmasphere, has provided new evidence of the dynamic and spatially-structured nature of the plasmasphere [*Sandel et al.*, 2001; *Burch et al.*, 2001]. The EUV global pictures fill in some of the observational gaps left by satellites in the past, facilitating comparison with models [*Goldstein et al.*, 2002b]. On 10 July 2000, EUV observed the effects of plasmaspheric erosion in a time series of global snapshots of the plasma-sphere. In this letter, we investigate the timing of this erosion event in relation to conditions in the solar wind (SW) and its imbedded interplanetary magnetic field (IMF).

2. EUV Observations of Erosion Event

[5] Between 4:25–9:32 UT on 10 July 2000, IMAGE EUV produced plasmasphere images from a vantage point near apogee. Figure 1a shows two snapshots of the helium plasmasphere, glowing in 30.4-nm light, taken at 5:06 and 8:00 UT by EUV. In the center of each image, which is a view from above the north pole, the apparent size and location of the Earth are indicated by the black circle. The Sun is to the upper right, in the direction of the white arrow. The bright arc at the Earth's dayside limb is airglow from neutral helium and O^+; a faint shadow extends antisunward from the Earth on the nightside. EUV consists of 3 cameras; the fields of view of the three cameras are joined to create a

[1]Department of Physics and Astronomy, Rice University, Houston, Texas, USA.
[2]Lunar and Planetary Laboratory, University of Arizona, Tucson, Arizona, USA.

0094-8276/03/2002GL016478$05.00

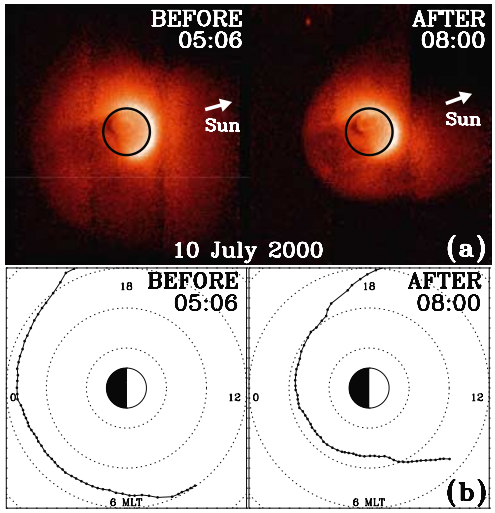

Figure 1. (a) Images of the He^+ plasmasphere taken by EUV at two times on 10 July 2000. (b) Plasmapauses from the EUV images above, mapped to the magnetic equatorial plane (Noon MLT to the right).

single image. The two faint vertical stripes bracketing the Earth are the edges of the cameras. Sunlight contamination in the rightmost camera shows up (especially at 8:00) as a blacked-out area in the upper right corner. (More details on the EUV instrumentation and interpretation of its images can be found in *Sandel et al.* [2000, 2001] and *Goldstein et al.* [2002a]) The plasmasphere is the bright red-orange haze of 30.4-nm light that surrounds the Earth. On the nightside, the plasmapause is the outer boundary where these 30.4-nm emissions drop off. On most of the dayside, the plasmapause is either outside the field of view, or obscured by sunlight contamination. Due to imperfect joining at the 3 camera edges, there is a small distortion of the plasmapause, where it crosses the camera edges; this does not affect the results plotted in Figures 2, 3 and 4.

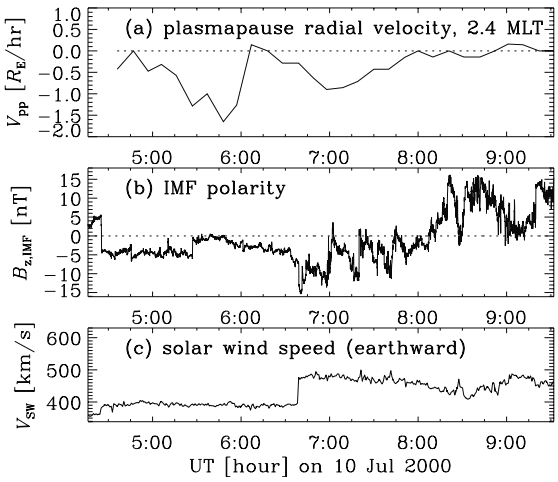

Figure 2. (a) Radial plasmapause velocity V_{pp} at 2.4 MLT, Inward motion occured in 2 bursts during 5–8 UT. (b) Propagation-delayed IMF z_{GSE}-component seen by Geotail MGF, showing 2 intervals of southward IMF. (c) V_{SW}, propagation-delayed earthward (GSE) component of solar wind velocity, seen by Geotail CPI.

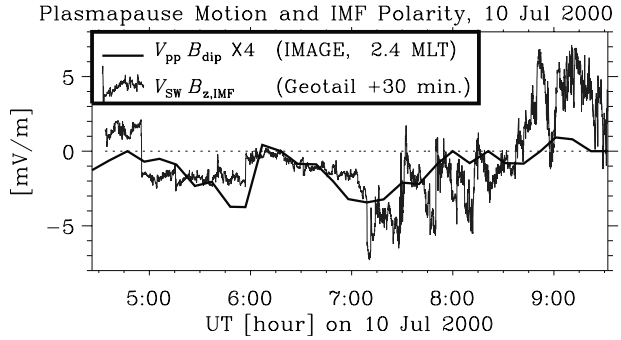

Figure 3. Electric field parameters $V_{pp}B_{dip}$ (plasmapause motion) and $V_{SW}B_{z,IMF}$ (IMF polarity). Correlation between the two curves was maximized (at 0.65) with 30-min delay added to Geotail data of Figure 2.

[6] In Figure 1b, the plasmapause of each image has been extracted and mapped down to the magnetic equator, with the Sun to the right. Comparing the plots at 5:06 and 8:00 UT, it is clear that the nightside plasmapause has moved inward by almost 2 R_E in 3 hours. Had this inward motion been due to a global compression, the plasmasphere (at a given location) would appear brighter in the 8:00 UT image than in the 5:06 UT image, since compression would make the interior density rise, and the image brightness is proportional to the line-of-sight-integrated helium density [*Sandel et al.*, 2000]. However, no such plasmaspheric brightening is evident, so the inward plasmapause motion must be due to erosion, i.e., stripping away of outer layers of the plasmasphere.

3. Analysis

[7] Although only two images ('before' and 'after') of the event are shown in Figure 1a, EUV observed the entire time sequence of the erosion, producing one image every 10–11 minutes. A plasmapause curve was extracted (as in Figure 1b) from each image between 4:25–9:32. Using the 31 plasmapause curves thus obtained, a 31-point time array of plasmapause radii R_{pp} was recorded at 2.4 MLT, the local time where the 5–6 UT plasmapause motion was most pronounced. This spot is unaffected by the camera-edge distortion mentioned in the last section. Centered time differencing of R_{pp} was used to calculate plasmapause radial velocity V_{pp} shown in Figure 2a. Inward plasmapause motion occurred in two distinct bursts within the 3-hour period 5–8 UT. The mean speed was 0.6 R_E/hour, and the total displacement −1.8 R_E. There is some jitter in measured values of V_{pp}, caused by finite error in the plasmapause extraction [*Goldstein et al.*, 2002a]; the uncertainty in V_{pp} is about ±0.3 R_E/hour.

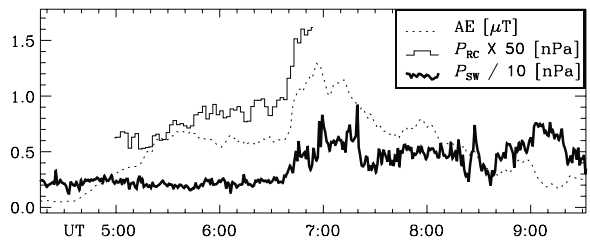

Figure 4. 10 July 2000 substorm index AE and ring current (RC) and solar wind (SW) pressure.

[8] IMF and solar wind conditions on 10 July 2000 were measured by the Geotail satellite's MGF [*Kokubun et al.*, 1994] and CPI [*Frank et al.*, 1994]. Figures 2b and 2c show, respectively, the IMF polarity ($B_{z,IMF}$, in nT) and the earthward SW speed (V_{SW}, in km/s). These data have been time-delayed by Δt_P = 3.7 minutes to account for propagation from Geotail's upwind position ($x_{GSE} \approx 24\ R_E$) to a nominal magnetopause (10 R_E), at speed $V_{SW} \approx 400$ km/s. The IMF x- and y- components (not shown) were >0 and ~constant (with a discontinuity at 6:45). There were 2 bursts of southward (S_{wd}) IMF within a 3-hour period beginning at 4:30 UT. By visual inspection alone, V_{pp} (panel a) and $B_{z,IMF}$ (panel b) have very similar time development, and seem to be correlated, with a time delay of $\Delta t_C \approx 30$ minutes (added to the propagation delay Δt_P). E.g., the first IMF turning is at 4:30 UT, and the erosion ensues at 5 UT.

[9] The solar wind and IMF impose an electric potential across the magnetosphere, driving convection ($E \times B$ drift of cold plasma). Therefore, when correlating plasmapause motion and southward IMF strength, it is meaningful to express them both in terms of quantities that have the units of electric (E) fields. Plasmapause motion can be represented by the E-field parameter $\varepsilon_P \equiv V_{pp}B_{dip}$, where B_{dip} is equatorial dipole geomagnetic field strength. The dipole field is smooth, so the variation of ε_P is qualitatively the same as V_{pp}. Similarly, $\varepsilon_{SW} \equiv V_{SW}B_{z,IMF}$. Other than a discontinuity at 6:40 V_{SW} is either roughly constant or slowly-varying (relative to $B_{z,IMF}$), so ε_{SW} varies (qualitatively) as $B_{z,IMF}$. Figure 3 compares ε_P and ε_{SW}. So that both plotted quantities are about the same magnitude, ε_P has been multiplied by 4. (E.g., the true magnitude of ε_P at 7:19 UT is about 0.8 mV/m.) To quantify the link between V_{pp} and $B_{z,IMF}$, we calculated the linear correlation coefficient between ε_P and ε_{SW}, with ε_{SW} delayed in time by Δt_C, for values of Δt_C between 0 and 90 minutes. The correlation peaks to a value of 0.65 that indeed occurs at Δt_C = 30 minutes. In Figure 3, ε_{SW} has been plotted with this 30-minute delay; the correlation between ε_P and ε_{SW} is visually apparent. Our interpretation of this correlation is that the solar wind is driving the plasmapause motion. The correlation peak at Δt_C = 30 minutes suggests that the coupling between the solar wind and the plasmasphere can take that long to occur. The close resemblance of V_{pp} to $B_{z,IMF}$ is consistent with the idea that in some sense the IMF polarity acts as a switch, turning convection on when the IMF turns southward.

4. Discussion

[10] Our interpretation is that the first erosion interval (~5–6 UT) resulted mainly from enhanced convection (triggered by the first S_{wd} IMF turning) that penetrated past the shielding layer. Convection is driven by the polar cap potential (PCP), which is determined by the response of the ionosphere to changes in the solar wind and IMF. Numerous observational studies have examined this ionospheric response (e.g., *Knipp et al.* [1991]; *Hairston and Heelis* [1995]; *Ridley et al.* [1998]; *Huang et al.* [2002]). From these results, at least 3 relevant time intervals can be defined. (1) Δt_P is the propagation time from solar-wind satellite to magnetopause MP. (2) Δt_B is the propagation time from MP to ionosphere (3–15 min.). (3) Δt_R is the time necessary to completely reconfigure ionospheric convection in response to changes in SW/IMF (10–25 min.). *Coroniti and Kennel* [1973] found theoretical value $\Delta t_R \approx$ 20 min., consistent with these observations. In the previous section we corrected for Δt_P and defined Δt_C, the time between arrival of S_{wd} IMF at the MP, and the start of plasmaspheric erosion. If we attribute delay Δt_C to ionospheric reconfiguration, then $\Delta t_C \equiv \Delta t_B + \Delta t_R$; our value Δt_C = 30 min is consistent with (2) and (3) above. This scenario implies 20–30 min lag between the S_{wd} IMF turnings in Figure 2b and the maximum value of PCP. Sparseness of DMSP-derived PCP data on 10 July precludes direct determination of the lag Δt_C, but future work on this event may use alternate techniques for estimating PCP (e.g., mentioned in *Ridley et al.* [1998]).

[11] The second erosion (~6:30–8 UT) probably arose from a combination of contributing effects, perhaps dominated by enhanced convection. For discussion, Figure 4 contains plots of the auroral electrojet (AE) index, an indicator of substorm activity (dotted line); P_{RC}, the average nightside pressure of 16–60 keV ring current protons (solid line); and P_{SW}, the solar wind dynamic pressure assuming 5% helium, delayed by Δt_P (heavy solid line). P_{RC} was deduced from observations by the IMAGE high energy neutral atom (HENA) imager [*Mitchell et al.*, 2000], via the inversion technique of *C:son Brandt et al.* [2002]. The onset of the 2nd erosion may have been hastened by magnetospheric compression. At 6:40–6:50 UT, erosion parameter ε_P seems to 'anticipate' the sharp negative trend in (Δt_C-delayed) ε_{SW} at 7:10. At 6:40, there occurred a 3- to 4-fold increase in P_{SW} that likely compressed the subsolar magnetopause to ~8.5 R_E. Although (as mentioned earlier) there was no measurable plasmaspheric compression in EUV images, major magnetospheric compressions can disrupt shielding [*Wolf et al.*, 1982] and/or create induction electric fields, causing erosion. Magnetic compression information reaches the nightside without reconfiguration delay Δt_R, so compression-induced erosion would precede PCP buildup (and convection) from the 3-fold $B_{z,IMF}$ magnitude increase at 6:40 UT (Figure 2). Consistent with this, the most notable feature of P_{RC} (Figure 4) is a sharp increase at 6:40, coincident with both the erosion enhancement and presumed compression. This post-6:40 enhanced RC may have participated in the creation of SAPS-like azimuthal flows in the pre-midnight sector [*Foster and Burke*, 2002] that contributed to the erosion process there. Preliminary analysis of DMSP data suggests this is a strong possibility [Foster, Spiro, private communications]. An induction E-field due to substorm dipolarization may have also contributed somewhat to the erosion. Substorm activity (given by AE in Figure 4) increased in phase with both erosion intervals, as is also evident in images from EUV, and from the IMAGE far ultraviolet (FUV) imager (not shown) [*Mende et al.*, 2000].

[12] There are indications that shielding was at least partially suppressed during much of the 10 July erosion. In Figure 2, the IMF turned abruptly southward at 4:30 UT, and stayed at ~5 nT for an hour. Had adequate shielding developed during this hour, the abrupt northward transition at 5:30 UT would not only reduce convection (and erosion) but would also trigger overshielding, moving the plasmapause outward ($V_{pp} > 0$). Instead, V_{pp} drops

very nearly to zero at 6:07 UT. This suggests that even after an hour of steady southward IMF, shielding was still incomplete. Effective shielding can be impeded by buildup of magnetic flux in the tail during an extended period of dayside reconnection [*Fejer et al.*, 1990]; a steady equatorward motion of the equatorward edge of the aurora would accompany this buildup. The general trend in both the auroral boundary index (ABI) [*Gussenhoven et al.*, 1983] and FUV imager data is a decrease from 65° to 60° during 4–8 UT, although there are 2°–4° equatorward excursions at ~5 and ~7 UT, possibly due to inward convective surges of the plasmasheet, in phase with the erosion intervals. Weak shielding may also explain why ε_P seems to follow the gradual southward trend of ε_{SW} from 6:07–6:39 UT (Figure 3), which otherwise might be slow enough (compared to the shielding time scale) to be shielded. Effective shielding requires adequate RC pressure. The P_{RC} increase from 5:15–5:50 is roughly in phase with the erosion activity (consistent with a convection interpretation), and its low value compared to the noise level (indicated by P_{RC} at 5 UT) is consistent with weak shielding during this time. Higher P_{RC} after 6:40 UT may have better shielded the plasmasphere, so that erosion began to taper off after 7:10. Weak shielding implies that compression-induced shielding disruption was not the dominant factor in the erosion, although it may have initiated the second erosion interval. Once begun, we suspect enhanced convection dominated the pre-dawn erosion process. Work is underway to quantify the role of pre-midnight azimuthal flows on 10 July.

5. Conclusion

[13] We have shown that the timing of observed inward motion of the plasmapause is significantly correlated to southward IMF turnings in the solar wind, with a time delay of 30 minutes. We suspect convection dominated the 10 July erosion, but the presence of other contributing effects including magnetopause compression, azimuthal flows, substorm activity and shielding suppression highlights the complexity of the coupling of the inner/outer magnetosphere, ionosphere, and solar wind. In principle, EUV data provide a means to estimate the E-field at the plasmapause [*Burch et al.*, 2001]. Analysis in this paper was limited to a single MLT along the moving plasmapause, but preliminary analysis at other MLT clearly indicates that the entire nightside plasmapause motion was correlated with the IMF. In future papers, we shall examine the global properties of plasmaspheric erosion and investigate more fully the importance of azimuthal flows at the flanks. The EUV observations of erosion events like 10 July will allow us to re-examine the simple long-standing ideas of plasmapause dynamics, including the global distribution of inner magnetospheric electric and flow fields.

[14] **Acknowledgments.** We gratefully acknowledge the data providers: T. Nagai, ISAS (Geotail MGF); K. Ackerson, L. Frank (Geotail CPI); P. Brandt (IMAGE HENA); World Data Center for Geomagnetism, Kyoto (AE); H. Frey, S. Mende (IMAGE FUV); F. Rich (ABI); M. Hairston (PCP). Discussions with D. Carpenter, R. Wolf and P. Brandt were extremely useful. We thank D. Gallagher for work on mapping EUV images to the equator. Work at Rice and Arizona was supported by NASA contract NAS5-96020 with SwRI, as part of the IMAGE mission.

References

Brice, N. M., Bulk motion of the magnetosphere, *J. Geophys. Res.*, *72*, 1967.
Burch, J. L., et al., Views of Earth's magnetosphere with the IMAGE satellite, *Science*, *291*, 619, 2001.
Carpenter, D. L., Earth's plasmasphere awaits rediscovery, *EOS Trans. AGU*, *76*, 89, 1995.
Carpenter, D. L., and R. R. Anderson, An ISEE/Whistler model of equatorial electron density in the magnetosphere, *J. Geophys. Res.*, *97*, 1097, 1992.
Chen, A. J., and R. A. Wolf, Effects on the plasmasphere of a time-varying convection electric field, *Planet. Space Sci.*, *20*, 483, 1972.
Coroniti, F. V., and C. F. Kennel, Can the ionosphere regulate magnetospheric convection?, *J. Geophys. Res.*, *78*, 2837, 1973.
C:son Brandt, P., et al., Global ENA observations of the storm mainphase ring current: Implications for skewed electric fields in the inner magnetosphere, *Geophys. Res. Lett.*, in press, 2002.
Fejer, B. G., R. W. Spiro, R. A. Wolf, and J. C. Foster, Latitudinal variation of perturbation electric fields during magnetically disturbed periods: 1986 SUNDIAL observations and model results, *Ann. Geophys.*, *8*, 441, 1990.
Foster, J. C., and W. J. Burke, SAPS: A new categorization for sub-auroral electric fields, *EOS Trans. AGU*, *83*, 393, 2002.
Frank, L. A., K. L. Ackerson, W. R. Pterson, J. A. Lee, M. R. English, and J. L. Pickett, The Comprehensive Plasma Instrumentation (CPI) for the Geotail spacecraft, *J. Geomagn. Geoelec.*, *46*, 23, 1994.
Goldstein, J., et al., Identifying the plasmapause in IMAGE EUV data using IMAGE RPI in situ steep density gradients, *J. Geophys. Res.*, in press, 2002a.
Goldstein, J., et al., IMF-driven overshielding electric field and the origin of the plasmaspheric shoulder of May 24, 2000, *Geophys. Res. Lett.*, *29*, 10.1029/2001GL014534, 2002b.
Gussenhoven, M. S., et al., Systematics of the equatorward diffuse auroral boundary, *J. Geophys. Res.*, *88*, 5692, 1983.
Hairston, M. R., and R. A. Heelis, Response time of the polar ionospheric convection pattern to changes in the north-south direction of the IMF, *Geophys. Res. Lett.*, *22*, 631, 1995.
Huang, T. S., R. A. Wolf, and T. W. Hill, Interchange instability of the Earth's plasmapause, *J. Geophys. Res.*, *95*, 17,187, 1990.
Huang, C.-S., et al., Effects of solar wind variations on the midlatitude ionosphere, *J. Geophys. Res.*, *107*, 10.1029/2001JA009025, 2002.
Kelley, M. C., B. G. Fejer, and C. A. Gonzales, An explanation for anomalous ionospheric electric fields associated with a northward turning of the interplanetary magnetic field, *Geophys. Res. Lett.*, *6*, 301, 1979.
Knipp, D. J., et al., Ionospheric convection response to changing IMF direction, *Geophys. Res. Lett.*, *18*, 721, 1991.
Kokubun, S., et al., The Geotail magnetic field experiment, *J. Geomagn. Geoelec.*, *46*, 7, 1994.
Lambour, R. L., et al., Global modeling of the plasmasphere following storm sudden commencements, *J. Geophys. Res.*, *102*, 24351, 1997.
LeDocq, M. J., D. A. Gurnett, and R. R. Anderson, Electron number density fluctuations near the plasmapause observed by the CRRES spacecraft, *J. Geophys. Res.*, *99*, 23661, 1994.
Lemaire, J. F. and K. I. Gringauz, *The Earth's Plasmasphere*, Cambridge University Press, Cambridge, 1998.
Mende, S. B., et al., Far ultraviolet imaging from the IMAGE spacecraft. 1, System design, *Space Sci. Rev.*, *91*, 243, 2000.
Mitchell, D. G., et al., High energy neutral atom (HENA) imager for the IMAGE mission, *Space Sci. Rev.*, *91*, 67, 2000.
Moldwin, M. B., et al., The fine-scale structure of the outer plasmasphere, *J. Geophys. Res.*, *100*, 8021, 1995.
Nishida, A., Formation of plasmapause, or magnetospheric plasma knee, by the combined action of magnetospheric convection and plasma escape from the tail, *J. Geophys. Res.*, *71*, 5669, 1966.
Richmond, A. D., Self-induced motions of thermal plasma in the magnetosphere and stability of the plasmapause, *Rad. Sci.*, *8*, 1019, 1973.
Ridley, A. J., et al., A statistical study of the ionospheric convection response to changing interplanetary magnetic field conditions using the assimilative mapping of ionospheric electrodynamics technique, *J. Geophys. Res.*, *103*, 4023, 1998.
Sandel, B. R., et al., The extreme ultraviolet imager investigation for the IMAGE mission, *Space Sci. Rev.*, *91*, 197, 2000.
Sandel, B. R., et al., Initial results from the IMAGE extreme ultraviolet imager, *Geophys. Res. Lett.*, *28*, 1439, 2001.
Wolf, R. A., et al., Computer simulation of inner magnetospheric dynamics for the magnetic storm of July 29, 1977, *J. Geophys. Res.*, *87*, 5949, 1982.

J. Goldstein and P. H. Reiff, Dept of Physics and Astron, Rice Univ, Houston, TX 77005, USA. (jerru@rice.edu)
B. R. Sandel and W. T. Forrester, Lunar and Planetary Lab, University of Arizona, Tucson, AZ 85721, USA.